Accepted Manuscript

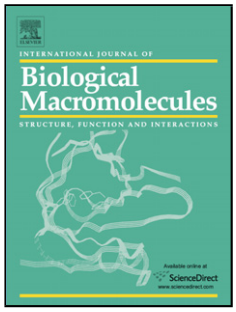

Title: Thermal stability of peroxidase from *Chamaerops excelsa* palm tree at pH 3

Authors: Laura S. Zamorano, Susana Barrera Vilarmau, Juan B. Arellano, Galina G. Zhadan, Nazaret Hidalgo Cuadrado, Sergey A. Bursakov, Manuel G. Roig, Valery L. Shnyrov

PII: S0141-8130(09)00018-X
DOI: doi:10.1016/j.ijbiomac.2009.01.004
Reference: BIOMAC 2407

To appear in: *International Journal of Biological Macromolecules*

Received date: 18-12-2008
Revised date: 15-1-2009
Accepted date: 16-1-2009

Please cite this article as: L.S. Zamorano, S.B. Vilarmau, J.B. Arellano, G.G. Zhadan, N.H. Cuadrado, S.A. Bursakov, M.G. Roig, V.L. Shnyrov, Thermal stability of peroxidase from *Chamaerops excelsa* palm tree at pH 3, *International Journal of Biological Macromolecules* (2008), doi:10.1016/j.ijbiomac.2009.01.004

Thermal stability of peroxidase from *Chamaerops excelsa* palm tree at pH 3.

Laura S. Zamorano [a,1], Susana Barrera Vilarmau [a,1,2], Juan B. Arellano [b], Galina G. Zhadan [c], Nazaret Hidalgo Cuadrado [a], Sergey A. Bursakov [d], Manuel G. Roig [a,*], Valery L. Shnyrov [c,*]

[a] *Departamento de Química Física, Facultad de Ciencias Químicas, Universidad de Salamanca, 37008 Salamanca, Spain*

[b] *Instituto de Recursos Naturales y Agrobiologia (IRNASA-CSIC), Apdo. 257, 37071 Salamanca, Spain*

[c] *Departamento de Bioquímica y Biología Molecular, Universidad de Salamanca, 37007 Salamanca, Spain*

[d] *Departamento de Protección Ambiental, Estacion Experimental del Zaidin (EEZ-CSIC), 18008 Granada, Spain*

[1]These authors contributed equally to this work.

[2]Present address: *Departamento de Ciencia de Proteinas, Centro de Investigaciones Biológicas, 28040 Madrid*

Abbreviations: CEP, palm tree - *Chamaerops excelsa* - peroxidase; CD, circular dichroism; DSC, differential scanning calorimetry.

* Corresponding authors. Tel.: +34 92 329 4465; fax: +34 92 329 4579.

E-mail address: shnyrov@usal.es (V.L. Shnyrov); mgr@usal.es (M.G. Roig)

Abstract

The structural stability of a peroxidase, a dimeric protein from palm tree *Chamaerops excelsa* leaves (CEP), has been characterized by high-sensitivity differential scanning calorimetry, circular dichroism and steady-state tryptophan fluorescence at pH 3. The thermally induced denaturation of CEP at this pH value is irreversible and strongly dependent upon the scan rate, suggesting that this process is under kinetic control. Moreover, thermally induced transitions at this pH value are dependent on the protein concentration, leading to the conclusion that in solution CEP behaves as dimer, which undergoes thermal denaturation coupled with dissociation. Analysis of the kinetic parameters of CEP denaturation at pH 3 was accomplished on the basis of the simple kinetic scheme $N \overset{k}{\rightarrow} D$, where k is a first-order kinetic constant that changes with temperature, as given by the Arrhenius equation; N is the native state, and D is the denatured state, and thermodynamic information was obtained by extrapolation of the kinetic transition parameters to an infinite heating rate.

Key words: Palm peroxidase; Protein stability; Differential scanning calorimetry; Circular dichroism; Fluorescence.

1. Introduction

Peroxidases (EC 1.11.1.7; donor: hydrogen peroxide oxidoreductase) are enzymes that are widely distributed in the living world and that are involved in many physiological processes. Although the function of peroxidases is often seen primarily in terms of effecting the conversion of H_2O_2 to H_2O, this should not be allowed to obscure their wider participation in other reactions, such as cell wall formation, lignification, the protection of tissues from pathogenic microorganisms, suberization, auxin catabolism, defense, stress, etc [1].

Peroxidases are important for various biotechnological purposes. This group of enzymes, in particular those from plants, enjoys widespread use as catalysts for phenolic resin synthesis [2,3], as indicators for food processing and diagnostic reagents [4,5] and as additives in bioremediation [6,7]. Under specific conditions the radicals formed can break bonds in polymeric materials resulting in their destruction, for instance, in lignin biodegradation [8]. Peroxidase has found an important application in the production of conducting polymers such as polyaniline [9,10]. Synthesis of polyaniline can occur in the presence of peroxidase, hydrogen peroxide as a reducing substrate, and sulfonated polystyrene and poly(vinyl-phosphonic acid) as polymeric templates at acidic (below 4) pH values [11]. Consequently, for the development of such biotechnological processes, it is of interest to find and characterize peroxidases that are stable under acidic conditions.

As with many enzymes, poor thermal and environmental stability limits the large-scale use of catalysis by peroxidases. This is particularly true in bioremediation and polyelectrolyte synthesis. Accordingly, the identification of highly stable and active peroxidases should be the first step in the development of a catalyst with broad

commercial and environmental appeal. Recently, peroxidases from the leaves of some tropical palm trees have been isolated and characterized [12-15]. These enzymes showed very high stability at elevated temperatures, within broad range of pH values, in the presence of hydrogen peroxide and chemical denaturants [16-18], that make them intriguing catalysts for industrial applications. Here we describe a detailed investigation of the thermal stability of peroxidase purified from leaves of cold-resistant palm tree *Chamaerops excelsa* at pH 3, by using different independent methods, such as differential scanning calorimetry (DSC), circular dichroism (CD), intrinsic fluorescence and enzymatic activity assays.

2. Materials and methods

2.1. Materials

Analytical or extra-pure grade polyethyleneglycol (PEG), guaiacol (2-methoxyphenol), ammonium sulfate, sodium phosphate and Tris-HCl were purchased from Sigma Chemical Co. (St. Louis, MO, USA) and were used without further purification. H_2O_2 was from Merck (Darmstadt, Germany). Superdex-200 columns and Phenyl-Sepharose CL-4B were from GE Healthcare Bio-Sciences AB (Uppsala, Sweden). Toyopearl DEAE-650 M was purchased from the Tosoh Corporation (Tokyo, Japan). Cellulose membrane tubing for dialysis (avg. flat width 3.0 in.) was purchased from Sigma Chemical Co.; slide-A-lyzer dialysis cassettes (extra-strength, 3-12 mL capacity, 10.000 MWCO) were from Pierce Biotechnology, Inc. (Rockford, IL, USA), and centrifuge filter devices (Amicon Ultra Cellulose 10.000 MWCO, 15 mL capacity) were from Millipore Corp. (Billerica, MA, USA). All other reagents were of the highest purity

available. The water used for preparing the solutions was double-distilled and then subjected to a de-ionisation process.

2.2. Enzyme Preparation

CEP was purified from palm tree *Chamaerops excelsa* leaves as described earlier [14].

The purity of the CEP was determined by SDS-PAGE, as described by Fairbanks et al. [19], on a Bio-Rad minigel device, using a flat block with a 15 % polyacrylamide concentration; by gel-filtration, performed using a Superdex 200 10/30 HR column connected to an ÄKTA-purifier system (GE Healthcare Bio-Sciences AB, Uppsala, Sweden) and by UV-visible spectrophotometry ($RZ \equiv A_{403}/A_{280} = 2.9 \pm 0.1$). Analytical isoelectrofocusing was performed on a Mini IEF cell model 111 (Bio-Rad Laboratories, Hercules, CA) using Ampholine PAG-plates, pH 3.5-9.5 (GE Healthcare Bio-Sciences AB, Upsala, Sweden). Electrophoretic conditions and Coomassie brilliant blue R-250 staining were as recommended by the manufacturer. The standards used were from a broad-range pI calibration kit (pH 4.45-9.6) from Bio-Rad Laboratories (Hercules, CA).

Protein concentrations were determined spectrophotometrically, using the experimentally determined extinction coefficient value at 403 nm for the protein monomer of 48.0 ± 0.5 $mM^{-1}cm^{-1}$.

Peroxidase activity toward guaiacol was measured spectrophotometrically at 25 °C. An aliquot of enzyme solution was added to a 1-cm spectral cuvette containing 18.1 mM guaiacol and 4.9 mM H_2O_2 in 20 mM sodium phosphate buffer, pH 6.0, in a final volume of 2 mL. The rate of change in absorbance due to substrate oxidation was

monitored at 470 nm. Peroxidase activities were calculated using a molar absorption coefficient of 5200 $M^{-1}cm^{-1}$ at 470 nm for the guaiacol oxidation product [20].

In titration experiments, pH values were adjusted by means of a polyethylene rod moistened with either 0.1 M HCl or 0.1 M NaOH.

2.3. Differential Scanning Calorimetry

Calorimetry scans were performed on a MicroCal MC-2D differential scanning microcalorimeter (MicroCal Inc., Northampton, MA, USA) with cell volumes of 1.22 mL as described previously [18,21,22,]. All solutions were degassed by stirring under a vacuum prior to scanning. An overpressure of 2 atm of dry nitrogen was always kept over the liquids in the cells throughout the scans. The reversibility of the thermal transitions was checked by examining the reproducibility of the calorimetric trace in a second heating of the sample immediately after cooling from the first scan. The molar excess heat capacity curves obtained by normalization with the protein concentrations and volume of the calorimeter cell were smoothed and plotted using the Windows-based software package (ORIGIN) supplied by MicroCal Inc. (Northampton, MA, USA). Analysis of the data was accomplished on the basis of:

1. The simple two-state irreversible model, $N_2 \overset{k}{\rightarrow} D$, where N_2 is the native dimer, D is the denatured monomer and k is the effective rate constant for the denaturation that changes with temperature, as given by the Arrhenius equation: $k = \exp[E_A(1/T^*-1/T)/R]$, where E_A is the energy of activation, and T^* is the temperature at which the rate constant equals 1 min^{-1}. In this case the excess heat capacity C_p^{ex} is given by the following equation [23]:

$$C_p^{ex} = \frac{1}{\nu}\Delta H \exp\left\{\frac{E_A}{R}\left(\frac{1}{T^*}-\frac{1}{T}\right)\right\} \times \exp\left\{-\frac{1}{\nu}\int_{T_o}^{T}\exp\left[\frac{E_A}{R}\left(\frac{1}{T^*}-\frac{1}{T}\right)\right]dT\right\} \quad (1)$$

where $\nu = dT/dt$ (K min^{-1}) is a scan rate value and ΔH is the enthalpy difference between the denatured and native states.

2. The two-state folding/unfolding reaction coupled with the model that corresponds to a situation in which the oligomeric protein made up of identical subunits obeys the equilibrium: $N_2 \overset{K}{\leftrightarrow} 2D$, where K is the equilibrium constant (see for details [18]).

2.4. Circular Dichroism

The far-UV CD spectra (190-250 nm) of CEP were recorded on a Jasco-715 spectropolarimeter (JASCO Inc., Easton, MD, USA) using a spectral band-pass of 2 nm and a cell path length of 1 mm. Protein concentrations of 0.1 to 0.2 mg mL^{-1} were used in these measurements. Five spectra were scanned for each sample at a scan rate of 50 nm min^{-1} and were then averaged. All spectra were background-corrected, smoothed, and converted to mean residue ellipticity $[\Theta] = 10\ M_{res}\ \Theta_{obs}\ l^{-1}\ p^{-1}$, where $M_{res} = 105$ is the mean residue molar mass, Θ_{obs} is the ellipticity (degrees) measured at wavelength - λ, l is the optical path-length of the cell (dm), and p is the protein concentration (mg/ml).

Thermal stability experiments were performed between 25 and 80 °C with a constant heating rate of 1 K min^{-1} using a Neslab RT-11 programmable water bath (Thermo Fisher Scientific, Inc., Waltham, MA, USA), and were followed by continuous measurements of ellipticity at 222 nm. Denaturation curves were transformed into the fractional degree of denaturation by the following equation, using a non-linear least

squares algorithm: $\theta = \theta_N (1 - \alpha) + \theta_D \alpha$, where $\theta_N = a_1 + a_2 x$ and $\theta_D = b_1 + b_2 x$ represent the mean values of ellipticity for the native and denatured conformations, respectively, obtained by linear regression of pre- and post-transitional baselines; x is the variable parameter.

2.5. Intrinsic Fluorescence

Steady-state fluorescence measurements were performed on a Hitachi F-4010 spectrofluorimeter (Hitachi Co., Ltd. Tokyo, Japan). Excitation was performed at 296 nm (with excitation and emission slit widths of 5 nm). The fluorescence measurements of CEP were carried out on protein solutions with an optical density of less than 0.2 at 280 nm to avoid the inner filter effect. All emission spectra were corrected for instrumental spectral sensitivity. The temperature dependence of the fluorescence intensity change at 360 nm with a heating rate of 1.8 K min^{-1} was investigated using thermostatically-controlled water circulating in a hollow brass cell-holder. Temperature in the sample cell was monitored with a thermocouple immersed in the cell under observation. Melting curves were transformed into the fractional degree of denaturation, as in the case of the CD measurements.

3. Results and discussion

3.1. Enzyme purification

CEP was purified to homogeneity with a high yield from palm tree *Chamaerops excelsa* leaves. The purification steps and their efficiencies are summarized in Table 1.

Purified peroxidase migrated in SDS-PAGE as a single band corresponding to a molecular weight of 50 ± 2 kDa (Fig. 1). The retention time of the elution of the protein from the size-exclusion column indicates that the enzyme forms dimers in solution with an approximate molecular weight of 109 ± 3 kDa (Fig. 2).

3.2. pH Dependence

To choose the most suitable pH conditions for stability studies, here we measured the pH dependence of the enzymatic activity and tryptophan fluorescence of CEP (Fig. 3). It is seen that CEP is a highly stable enzyme over a pH-range - from pH 2.5 to 6.0 - without any significant changes in the enzymatic activity and fluorescence parameters. Thus, one of the most useful parameters of the protein fluorescence spectrum - its maximum position, which reflects the degree of accessibility of the chromophores to solvent molecules [24] - remains constant (variation in limits of ± 0.2 nm) within a pH-range from about 2.8 to 6. This implies that the accessibility of the CEP tryptophan side chains to water molecules remains essentially invariant in this pH range. Furthermore, the fluorescence intensity did not change, indicating the absence of changes in the fluorescence quenching properties of the tryptophan environment in this pH-range. Thus, the pH range from 3 up to 6, characterized by the absence of evident pH-dependent fluorescence changes, seems to be the correct range of choice for the physico-chemical characterization of CEP. Acidification of the protein solution down to a pH below 2 caused a 3.6 nm red shift in the fluorescence spectrum, followed by a blue shift below pH 1.5, brought about by protein aggregation and a marked (more than four-fold) increase in fluorescence intensity. Comparison of these changes with the changes in enzymatic activity indicates that only the fluorescence intensity reflects acidic

denaturation of CEP, while the position of the fluorescence spectrum, reflecting the polarity of the tryptophan side chain environment, shows that polarity is not relevant for the enzymatic function of CEP.

3.3. DSC

The thermal denaturation of CEP at pH 3.0 gave rise to well defined DSC transitions whose values of temperatures of the excess heat capacity maximum (T_m) were dependent on the temperature scan rate. This effect can be seen in Fig. 4, which shows the thermal transitions for CEP at four different scan rates. The thermal denaturation of CEP under these experimental conditions was always calorimetrically irreversible since in a second heating of the enzyme solution no thermal effect was observed. All this clearly indicates that the observed thermal transitions characterize an irreversible, kinetically controlled process. Since, following the data of size exclusion chromatography, CEP forms dimers in solution, thermally induced denaturation should be accompanied by its dissociation into subunits, which should produce a concentration dependence of T_m [25-27]. In fact, the T_m and ΔH_{cal} values for the thermal denaturation of CEP at pH 3.0 were found to be dependent on the protein concentration within the 0.4 – 2.6 mg mL^{-1} range (data not shown), T_m increasing up to 1.1 degrees, and ΔH_{cal} up to 2%. The ratio of the van 't Hoff and calorimetric enthalpies obtained at different concentrations and different scan rates averaged 1.36 ± 0.08, fairly close to the value calculated with equation: $\frac{\Delta H_{VH}}{\Delta H(T_m)} = \frac{2 \cdot n}{n+1}$, which is valid for the case when the denaturation of oligomeric proteins is coupled to their dissociation into monomers [26]: i.e., 1.333 for dimer. Accordingly, despite a very small variation in the kinetic parameters of CEP denaturation with concentration, in all the experiments performed at

this pH we used the same concentration of protein to be sure that results obtained in different experiments would be concentration independent. Analysis of the DSC transitions under these conditions was accomplished on the basis of a simple two-state irreversible model $N_2 \overset{k}{\rightarrow} D$ (see Materials and Methods). It should be noted that a realistic model of protein denaturation in this case should include two steps: reversible unfolding and irreversible alteration of the unfolded state to produce the final denatured state, which is unable to fold back to the native protein. This scheme, usually known as the Lumry-Eyring model [28] in case of dimeric proteins, can be depicted as: $N_2 \underset{k_{-1}}{\overset{k_1}{\leftrightarrow}} 2U \overset{k_d}{\rightarrow} D$, where N_2 is the native dimer, U is the unfolded monomer, D is the irreversibly denatured monomer, k_1 and k_{-1} are the rate constants for the forward and reverse unfolding process with concomitant dissociation, and k_d is the rate constant for the denaturation of the monomers. However, use of the whole Lumry-Eyring model for the quantitative description of thermally induced transitions is difficult because the corresponding system of differential equations does not have an analytical solution at varying temperatures. It is therefore necessary to evaluate simpler mathematical models that are particular cases of the whole Lumry-Eyring model. In the present work we used the model that includes only one irreversible step, assuming that monomer denaturation is rapid in comparison with the dissociation of the dimer and the association of monomers, i. e. $k_d \gg k_1$ and $k_d \gg k_{-1}$. This means that the thermally induced disruption of the quaternary structure of the dimer adheres kinetically to the "all-or-not" law: $N_2 \overset{k}{\rightarrow} D$.

The excess heat capacity functions obtained for CEP in this case were analyzed by fitting the data to the two-state irreversible model - equation (1) - either individually or globally, using scan rate as an additional variable. The results of the fitting are shown

in Fig. 4 (solid lines) and in Table 2. As can be seen, when fitting was carried out both separately on the individual experimental curves and simultaneously on all the curves, a good approximation was achieved. Attempts to include different irreversible models for CEP denaturation - the Lumry-Eyring model, with a fast equilibrating first step, and the model that includes two consecutive irreversible steps [29,30] - did not improve the goodness of the fit, indicating that the two-state irreversible model is sufficient to quantitatively describe the kinetics of CEP denaturation. This conclusion was further confirmed by our spectral investigation on the thermal denaturation of this enzyme.

It is clear that equilibrium thermodynamics cannot be applied directly in the analysis of CEP denaturation at pH 3 because of its kinetically controlled nature. However, it is possible to obtain useful thermodynamic information upon extrapolation of the transition parameters to the infinite heating rate [31]. The thermodynamic parameters obtained in this manner for the thermal denaturation of CEP at pH 3 are shown in Table 2. If it is taken into account that in the acid pH range ion pairs, which are known to be important for the stability of haeme-containing class III peroxidases [32], have disappeared due to protonation that it may be assumed that value of the standard free energy change for CEP at neutral pH may be 5 – 10 kcal mol^{-1} higher [18,33] demonstrating that this enzyme is extremely stable.

3.4. CD Experiments

The CD spectra of intact and thermally denatured CEP at pH 3 are shown in Fig. 5A. A detailed secondary structure analysis of the CD spectra was performed using the CDPro software package [34]. The experimental data in 190-240 nm range were subjected to treatment by three programs included in this software package -

SELCON3, CDSSTR, and CONTINLL - using the SP43 (for intact proteins) and SDP48 (for denatured proteins) reference sets. The lowest root mean square deviation (RMSD) between the experimental data and the theoretical curves produced by the programs with these reference sets was obtained with CDSSTR, and hence the results obtained with SELCON3 and CONTINLL were omitted. The results of this analysis are given in Table 4. The values thus obtained for intact CEP are typical of different heme peroxidases [35]. It should be noted here that the estimates for the β-sheet and β-turn are usually worse than the estimate for the α-helix because the intensities of the β structure elements are lower than those of the α-helix [36].

Upon heating the CEP up to the denaturation temperature, the shape of the spectrum changed, pointing to an increase in the unordered structure, mainly at the expense of the α-helical structure (see Table 4). The increase in the quantity of β-strands that also occurred in denatured CEP indicates that this form of the enzyme undergoes some aggregation, most probably with an intramolecular character, because we failed to detect an increase in turbidity in the denaturation process.

The thermal denaturation of CEP was monitored by following the changes in molar ellipticity at 222 nm since at this wavelength the changes in ellipticity are significant upon enzyme denaturation. With increasing temperature (Fig. 5B), an irreversible cooperative transition to the denatured state occurred, which was analyzed by using a non-linear least squares fitting to Eq. (2) (see line through the data points):

$$F_{\mathrm{d}} = 1 - \exp\left\{ -\frac{1}{\nu} \int_{T_{\mathrm{o}}}^{T} \exp\left[\frac{E_{\mathrm{A}}}{R} \left(\frac{1}{T^*} - \frac{1}{T} \right) \right] dT \right\} \qquad (2)$$

where F_{d} refers to the denatured fraction [23]. This fitting affords the T^* parameter and the activation energy for CEP. These values are 344.4±0.3 K and 103.2 ± 1.7 kcal mol^{-1},

respectively, which are similar to those observed for the same parameters obtained by DSC (Table 2).

3.5. *Fluorescence Experiments*

Environmental changes in aromatic side chains resulting from conformational changes in the tertiary structure of proteins were measured by intrinsic fluorescence spectroscopy. Fig. 5C shows the fluorescence spectra of intact (solid line) and thermally denatured (dashed line) CEP at pH 3.0, excited at 296 nm. The fluorescence emission of the intact CEP has a very low quantum yield due to energy transfer to the heme which, as can be seen in Fig. 5C, essentially increases in the denatured enzyme owing to a change in the relative orientation or distance between the heme and the tryptophan residue(s) [37]. In view of these results, we used the changes in fluorescence intensity to analyze the effect of heating on the CEP denaturation process. On increasing temperature (Fig. 5D), an irreversible cooperative transition to the denatured state occurred, which was analyzed by non-linear least squares fitting to the equation (2). This fitting (solid line in Fig. 5D) afforded values of T^* = 343.9 ± 0.4 K and E_A = 102.9±2.3 kcal mol^{-1}, which are in satisfactory agreement with the values obtained from DSC and CD experiments (see above).

4. Conclusions

On comparing the kinetic parameters of CEP stability at pH 3 with those of other peroxidases [17,18,21,22], it is evident that that the thermostability of CEP is substantially greater than that of horseradish peroxidase isoenzyme *c* (HRP*c*) and anionic peanut (*Arachis hypogaea* L.) peroxidase (aPrx), and is practically the same as

the stability of peroxidase from the African oil palm tree *Elaeis guineensis* (AOPTP) and peroxidase from royal palm tree *Roystonea regia* (RPTP). Thus, the T_m for CEP at a scan rate of 60 K h^{-1} is 70.1 ± 0.2 °C while for aPrx this value is 39.4 ± 0.2 °C; for HRP*c* it is 60.2 ±0.2 °C; for AOPTP it is 72.3 ± 0.2 °C and for RPTP it is 72.3 ± 0.2 °C. In row of the Arrhenius energy of activation values CEP (105.1 ± 1.7 kcal mol^{-1}) close to AOPTP (103 ± 6 kcal mol^{-1}) being lower RPTP (129.1 ± 0.8 kcal mol^{-1}) and significantly higher in comparison those of HRPc (38.2 ± 0.5 kcal mol^{-1}) and aPrx (67.9 ± 0.5 kcal mol^{-1}). Obviously leaves of palm trees are the best source of the most structurally and functionally stable peroxidases pointing to their great potentiality for different biotechnological applications.

Acknowledgments

This work was partially supported by projects SA-06-00-0 ITACYL-Universidad de Salamanca and SA 129A07 (Junta de Castilla y León) and BFU2004-01432 and BFU2007-68107-C02-02/BMC (Ministerio de Educación y Ciencia) Spain. L.S.Z was fellowship holders from the Junta de Castilla y León, Spain (Ref. EDU/1490/2003).

References

1. C. Penel, T. Gaspar, H. Greppin, Plant Peroxidases 1980-90. Topics and Detailed Literature on Molecular, Biochemical, and Physiological Aspects. University of Geneva, Switzerland 1992.
2. J.S. Dordick, M.A. Marletta, A.M. Klibanov, Biotechnol. Bioeng. 30 (1987) 31-36.
3. J.A. Akkara, K.J. Senecal, D.L. Kaplan, J. Polym. Sci: Part A: Polymer Chemistry 29 (1991) 1561-1574.
4. Q.R. Thompson, Anal. Chem. 59 (1987) 1119-1121.
5. Z. Weng, M. Hendrickx, G. Maesmans, P. Tobback, J. Food Sci. 56 (1991) 567-570.
6. D. Arseguel, M. Baboulène, J. Chem. Technol. Biotechnol. 61 (1994) 331-335.
7. P.R. Adler, R. Arora, A. El Ghaouth, D.M. Glenn, J.M. Solar, J. Environ. Qual. 23 (1994) 1113-1117.
8. D. Cullen, P.J. Kersten, Enzymology and molecular biology of lignin degradation, in: The Micota III – Biochemistry and Molecular Biology (R. Brambl and G.A. Mazzluf, eds) pp. 249-273, Springer-Verlag, Berlin-Heidelberg, 2004.
9. A.V. Caramyshev, E.G. Evtushenko, V.F. Ivanov, A. Ros Barceló, M.G. Roig, V.L. Shnyrov, R.B. van Huystee, I.N. Kurochkim, A.K. Vorobiev, I.Y. Sakharov, Biomacromolecules 6 (2005) 1360-1306.
10. A.V. Caramyshev, V.M. Lobachev, D.V. Selivanov, E.V. Sheval, A.K. Vorobiev, O.N. Katasova, V.Y. Polyakov, A.A. Makarov, I.Y. Sakharov, Biomacromolecules 8 (2007) 2549-2555.

11. W. Liu, J. Kumar, S. Treipathy, K.J. Senecal, L. Samuelson, J. Am. Chem. Soc. 121 (1999) 71-78.

12. I.Y. Sakharov, J. Castillo Leon, J.C. Ariza, I.Y. Galaev, Bioseparation 9 (2000) 125-132.

13. I.Y. Sakharov, M.K. Vesga, I.Y. Galaev, I.V. Sakharova, O.Y. Pletjushkina, Plant Sci. 161 (2001) 853-860.

14. L. Watanabe, A.S. Nascimento, L.S. Zamorano, V.L. Shnyrov, I. Polikarpov, Acta Cryst. F63 (2007) 780-783.

15. G.H. Onsa, N. bin Saari, J. Selamat, J. Bakar, Food Chem. 85 (2004) 365-376.

16. I.Y. Sakharov, I.V. Sakharova, Biochim. Biophys. Acta 1598 (2002) 108-114.

17. A. Rodríguez, D.G. Pina, B. Yélamos, B., J.J. Castillo Leon, G.G. Zhadan, E. Villar, F. Gavilanes, M.G. Roig, I.Y. Sakharov, V.L. Shnyrov, Eur. J. Biochem. 269 (2002) 2584-2590.

18. L.S. Zamorano, D.G. Pina, J.B. Arellano, S.A. Bursakov, A.P. Zhadan, J.J. Calvete, L. Sanz, P.R. Nielsen, E. Villar, O. Gavel, M.G. Roig, L. Watanabe, I. Polikarpov, V.L. Shnyrov, Biochimie 90 (2008) 1737- 1749.

19. G. Fairbanks, T. Steck, D.F.N. Wallach, Biochemistry 10 (1971) 2606-2617.

20. A. Lindgren, T. Ruzgas, L. Gorton, E. Csöregi, G.B. Ardila, I.Y. Sakharov, I.G. Gazaryan, Biosens. Bioelectron. 15 (2000) 491-497.

21. D.G. Pina A.V. Shnyrova, F. Gavilanes, A. Rodríguez, F. Leal, M.G. Roig, I.Y. Sakharov, G.G. Zhadan, E. Villar, V.L. Shnyrov, Eur. J. Biochem. 268 (2001) 120-126.

22. L.S. Zamorano, D.G. Pina, F. Gavilanes, M.G. Roig, I.Y. Sakharov, A.P. Jadan, R.B. van Huystee, E. Villar, V.L. Shnyrov, Thermochim. Acta 417 (2004) 67-73.

23. B.I. Kurganov, A.E. Lyubarev, J.M. Sanchez-Ruiz, V.L. Shnyrov, Biophys. Chem. 69 (1997) 125-135.

24. E.A. Permyakov, Luminescent spectroscopy of proteins. Boca Raton: CRC Press, 1993.

25. S.P. Manly, K.S. Matthews, J.M. Sturtevant, Biochemistry 24 (1985) 3842-3846.

26. E. Freire, Comm. Mol. Cell. Biophys. 6 (1989) 123-140.

27. J.M. Sanchez-Ruiz, Biophys. J. 61 (1992) 921-935.

28. R. Lumry, H. Eyring, J. Phys. Chem. 58 (1954) 110-120.

29. A.E. Lyubarev, B.I. Kurganov, Biochemistry (Moscow) 63 (1998) 434-440.

30. A.E. Lyubarev, B.I. Kurganov, Biochemistry (Moscow) 64 (1999) 832-838.

31. P.L. Privalov, S.A. Potekhin, Methods Enzimol. 131 (1986) 4-51.

32. J.W. Tams, K.G. Welinder, Biochemistry 35 (1996) 7573-7579.

33. M. Sawano, H. Yamamoto, K. Ogasahara, S. Kidokoro, S. Katoh, T. Ohnuma, E. Katoh, S. Yokoyama, K. Yutani, K. Biochemistry 47 (2008) 721-730.

34. N. Sreerama, S.Y. Venyaminov, R.W. Woody, Protein Sci. 8 (1999) 370-380.

35. L. Banci, J. Biotechnol. 53 (1997) 253-263.

36. S.Y. Venyaminov, J.T. Yang, Determination of protein secondary structure, in: Circular Dichroism and the Conformational Analysis of Biomolecules (G.D. Fasman, ed) pp. 69-107, Plenum Press, New York, 1996.

37. B.C. Hill, P.M. Horowitz, N.C. Robinson, Biochemistry 25 (1986) 2287-2292.

Figure legends

Fig. 1. SDS-PAGE analysis of CEP (lane 3). Lane 2 contains for comparison royal palm tree peroxidase [18] and lane 1 contains molecular-weight markers from Novex Sharp Pre-Stained Standards (Invitrogen Co.) - from top to bottom: 260 kDa, 160 kDa, 110; 80 kDa, 60 kDa, 50 kDa, 40 kDa, 30 kDa, and 20 kDa.

Fig. 2. High-performance gel filtration of CEP on Superdex 200 HR 10/30 at a flow rate of 0.4 ml min^{-1}. The solid line is the absorbance at 403 nm and the dashed line is that at 280 nm. The insert shows calibration line for the standard proteins from LMW Calibration Kit (GE Healthcare) on Superdex 200 10/30 HR column: 1 – dimer of conalbumin (150 kDa), 2 – dimer of ovalbumin (86 kDa), 3 – conalbumin (75 kDa), 4 – ovalbumin (43 kDa), 5 – carbonic anhydrase (29 kDa), 6 – dimer of ribonuclease A (27.4 kDa), 7 – ribonuclease A (13.7 kDa) and 8 – aprotinin (6.5 kDa).

Fig. 3. pH-dependence of enzymatic activity (A) and fluorescence parameters (B) of CEP at 25 °C. Measurements were performed in 10 mM universal buffer (CH_3COOH, H_3PO_4, H_3BO_3-NaOH) with a protein concentration of ca. 10 μM. Activity was measured toward guaiacol. Open circles in (B) represent fluorescence intensity (arbitrary units) at 350 nm, which is proportional to the fluorescence quantum yield, and closed circles correspond to the position of the maximum of the fluorescence spectrum λ_{max}. The excitation wavelength was 296 nm.

Fig. 4. Temperature dependence of the excess molar heat capacity of CEP at scan rates of 29.7 K h^{-1} (squares), 45.5 K h^{-1} (triangles), 59.3 K h^{-1} (circles) and 87.5 K h^{-1}

(diamonds) in 20 mM citrate buffer, pH 3.0. Solid lines represent the best fit to each experimental curve using equation (1). The protein concentration was 23.9 μM.

Fig. 5. Thermally induced denaturation of CEP studied by optical spectroscopy. (A) Far-UV CD spectra of intact CEP at 25 °C (open circles) and thermally denatured CEP at 80 °C (closed circles) at pH 3.0 and protein concentration of 10.2 μM. The solid lines through the symbols are the best fits to the experimental data with the CDSSTR program, using SP43 for the intact and SDP48 for denatured protein as reference sets. (B) Fractional degree of thermal unfolding of CEP as a function of temperature, at pH 3.0, monitored by the changes in ellipticity at 222 nm, obtained upon heating at a constant scan rate of 60.3 K h^{-1}. The solid line represents the theoretical curve resulting from fitting the experimental data to the two-state irreversible model using Eq. (2). (C) Fluorescence spectra of intact - at 25 °C (solid line) and thermally denatured at 80 °C (dashed line) - CEP at pH 3.0 and protein concentration of 17.9 μM. The excitation wavelength was 296 nm. (D) Fractional degree of thermal unfolding of CEP as a function of temperature monitored by the changes in fluorescence intensity at 360 nm at pH 3.0, obtained upon heating at a constant scan rate of 108.3 K h^{-1}. The solid line represents the best fit obtained using Eq. (2).

Table 1

Purification steps of CEP

Procedure	Volume (ml)	Protein (mg)	Total activity[a] (U)	Specific activity[a] (U mg^{-1})	Purification	Yield (%)
Homogenate	6020	27515	211469	7.7	1	100
PEG + $(NH_4)_2SO_4$	2750	9466	199898	21.1	3	95
Phenyl-Sepharose	54	662	138230	209.9	27	66
DEAE-Toyopearl	2.5	27	79879	2925.9	380	38
Superdex 200	20	11	69231	6293.7	817	33

[a] The enzyme activity was measured toward guaiacol

Table 2

Arrhenius equation parameter estimates for the two-state irreversible model of the thermal denaturation of CEP at pH 3. The correlation coefficient (r) was calculated as $r = \sqrt{1 - \sum_{i=1}^{n}\left(y_i - y_i^{calc}\right)^2 / \sum_{i=1}^{n}\left(y_i - y_i^{m}\right)^2}$, where y_i and y_i^{calc} are respectively the experimental and calculated values of C_p^{ex}; y_i^{m} is the mean of the experimental values of C_p^{ex} and n is the number of points

Parameter	Temperature scan rate (K h^{-1})				Global fitting
	29.7	45.5	59.3	87.5	
ΔH (kcal mol^{-1})	119.4 ± 1.6	128.4 ± 1.9	130.2 ± 1.9	131.1 ± 2.1	
T^* (K)	345.0 ± 0.1	344.8 ± 0.2	345.1 ± 0.1	344.8 ± 0.2	345.0 ± 0.2
E_A (kcal mol^{-1})	107.3 ± 1.2	103.9 ± 1.4	103.3 ± 1.3	104.8 ± 1.4	106.2 ± 1.6
r	0.9996	0.9995	0.9995	0.9992	0.9989

Table 3

Thermodynamic parameters for the thermal denaturation of CEP at pH 3

T_m (°C)	$T_{1/2}$ (°C)	T_o (°C)	$\Delta H(T_m)$ (kcal mol^{-1})	T_s (°C)	$\Delta G^o(T_s)$ (kcal mol^{-1})
71.8	70.4	80.7	131.2	21.7	13.6

The standard deviation for T_m and $T_{1/2}$ values is ±0.2 K; the enthalpy of the denaturation was determined by extrapolation of experimentally determined transition parameters to the infinite heating rate with a standard deviation of ±5%; T_o is the temperature value at which change of the standard free energy $\Delta G^o(T) = \Delta H(T_{1/2})\,(1 - T/T_o) - \Delta C_p\,[(T_o - T) + T\ln(T/T_o)] \equiv 0$ and $\Delta C_p = 2.4 \pm 0.3$ kcal K^{-1} mol^{-1} was obtained from the difference in heat capacity between the native and denatured states of the protein at the transition mid point. T_s is the temperature of maximum stability.

Table 4

Secondary structure elements (%) determined from analysis of the CD spectra for intact and denatured CEP at pH 3

Protein	α-Helix			β-Strand			β-Turn	Unordered
	Regular	Distorted	Total	Regular	Distorted	Total		
Intact	20	18	38	0	7	7	22	33
Denatured	4	6	10	19	9	28	15	47

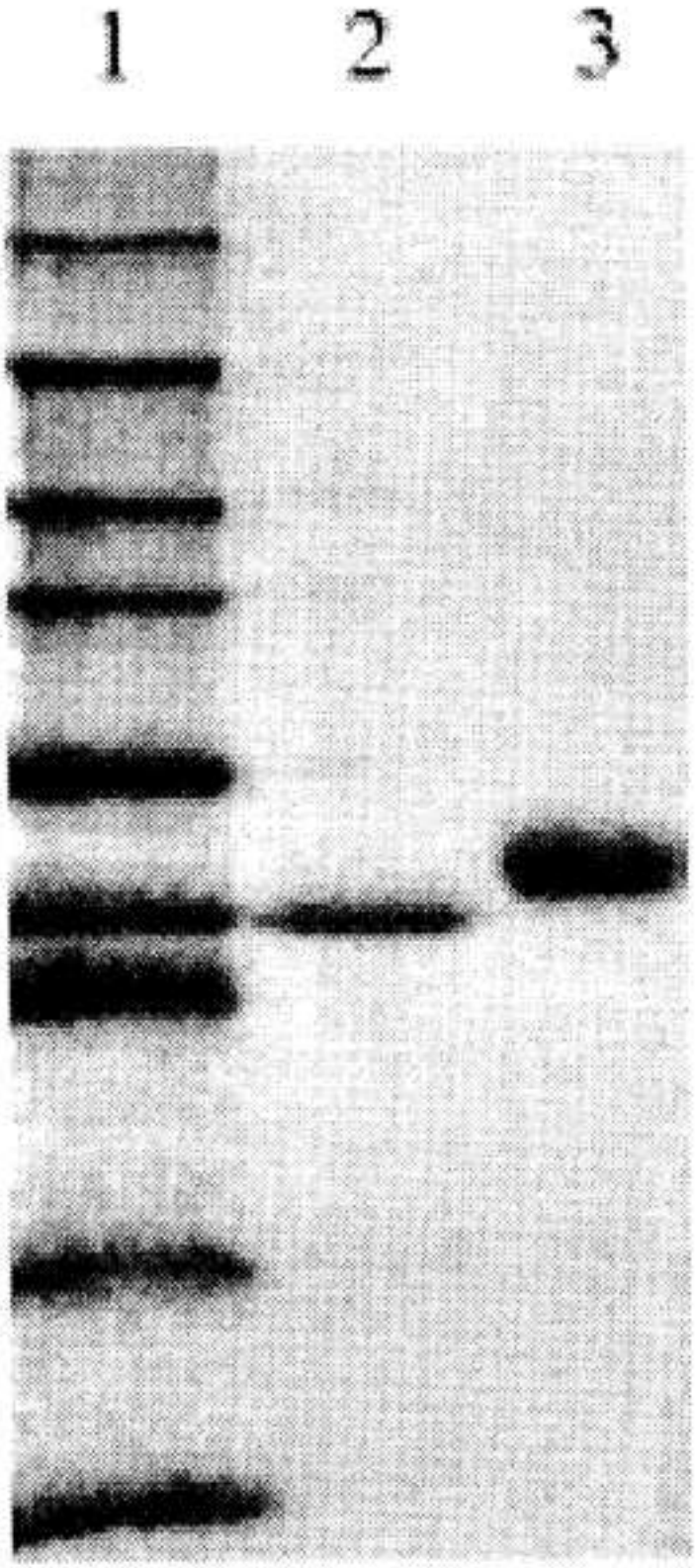

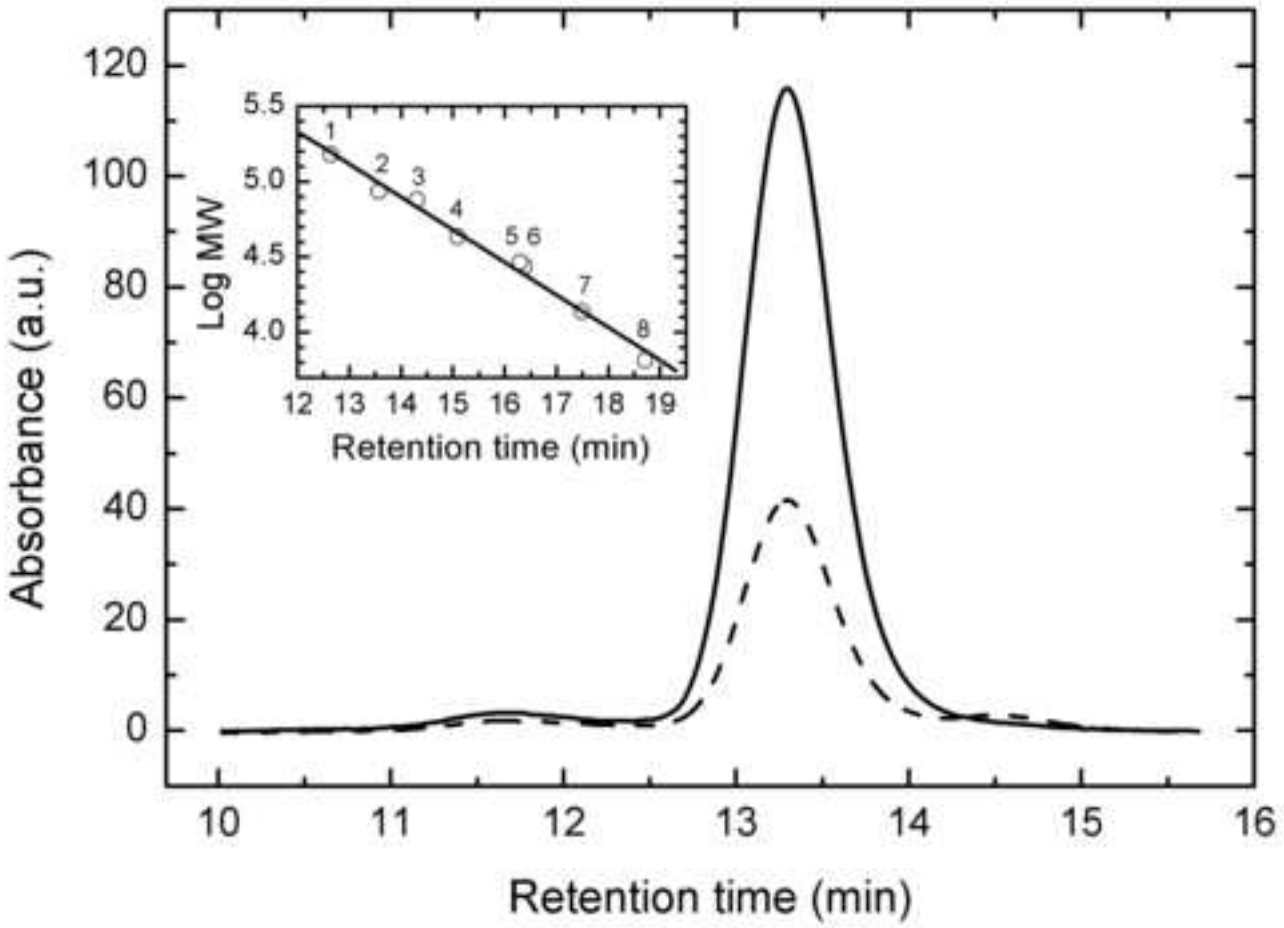

Figure 2

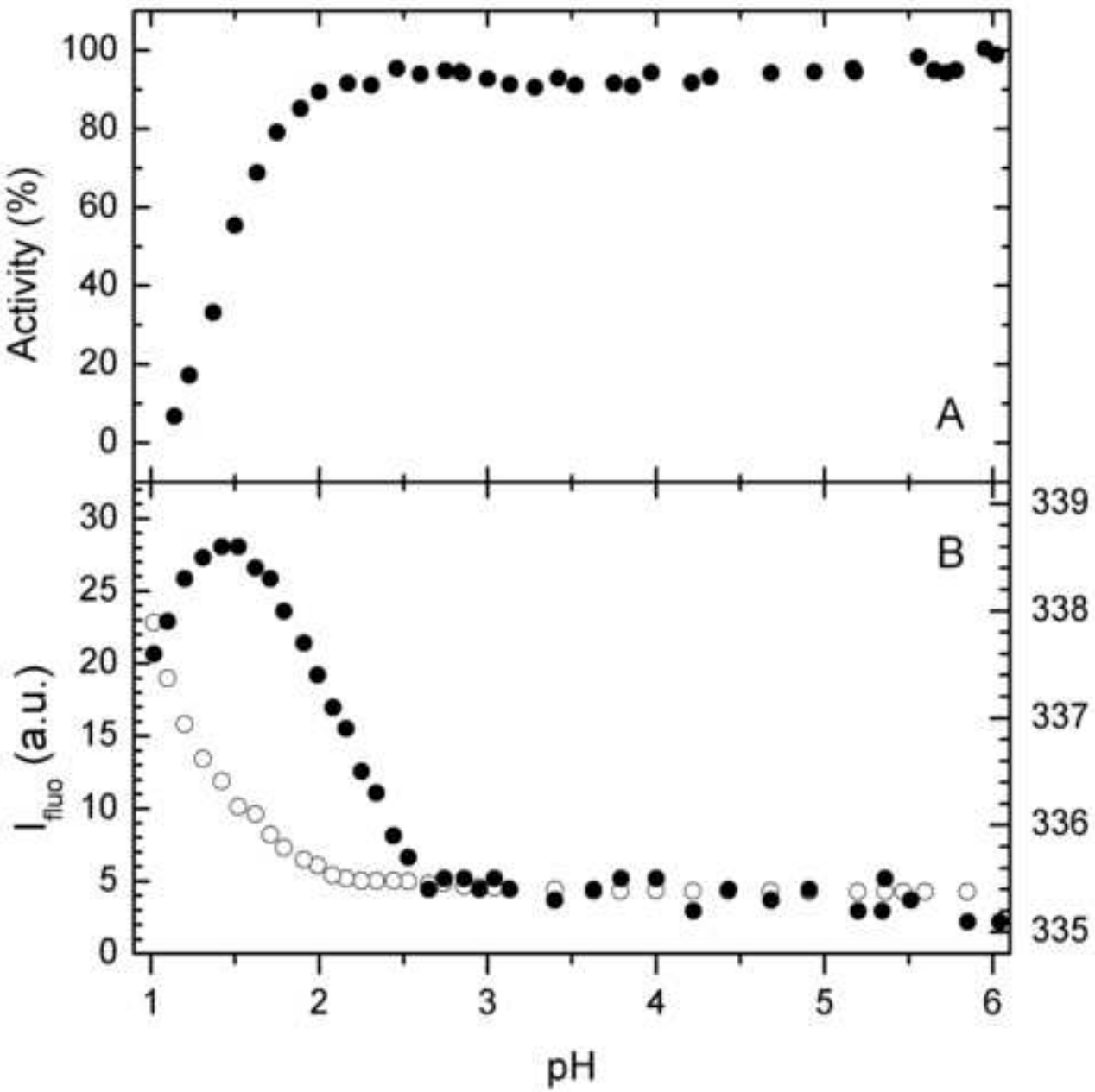

Figure 3

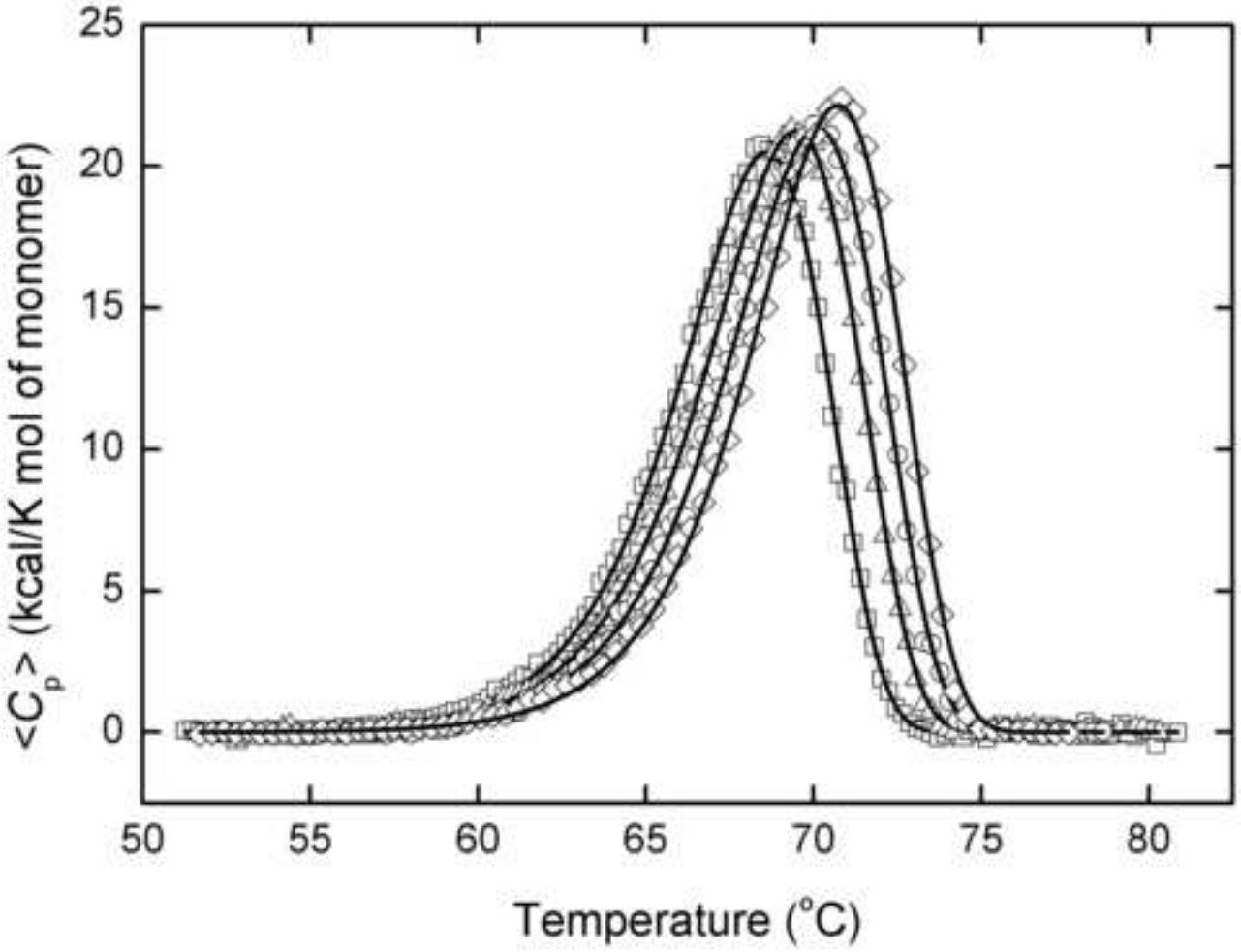

Figure 4

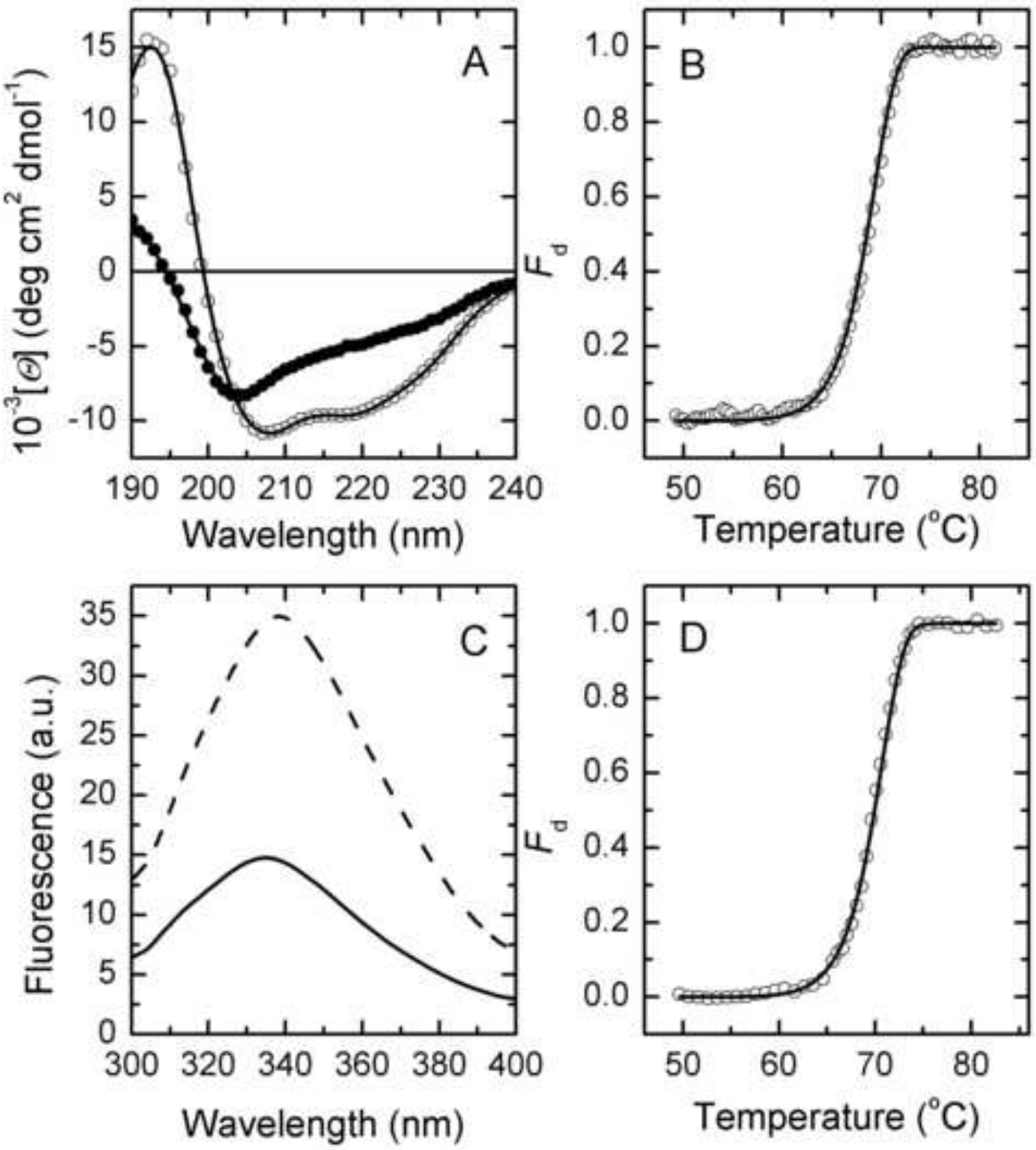

Figure 5